NOTICE CONCERNING COPYRIGHT RESTRICTIONS

Geothermal Resources Council, TRANSACTIONS, Vol. 11, October 1987

HYDRAULIC AND THERMAL BEHAVIOR OF A HOT DRY ROCK RESERVOIR DURING A 30-DAY CIRCULATION TEST

Sharad Kelkar[1], Zora Dash[1], Mark Malzahn[2], and Robert Hendron[1]

[1]Los Alamos National Laboratory, Los Alamos, New Mexico
[2]Contractor, Los Alamos, New Mexico

ABSTRACT

Testing has been in progress since January 1985 in the second Hot Dry Rock reservoir located at Fenton Hill, New Mexico. The results of a 30-day circulation test, conducted in 1986, are reported. The nominal reservoir depth is 3,650 m (11,750 ft) and the mean in situ temperature of the reservoir is 245°C. During the test 37,000 m^3 (9.76 million gal) of cold water was injected into the reservoir and hot water was recovered at temperatures ranging up to 192°C. This corresponded to a maximum thermal power output of about 10 MW_t. About 66% of the injected water was recovered during this test and a further 20% was recovered during a subsequent vent. The produced fluid's flow rate, temperature and power increased throughout the test. Assuming these trends continue, energy production rates around 12 MW_t at the end of one year can be expected. The results of the test show that future efforts for performance improvement need to be focused on the production well.

I. INTRODUCTION

A 30-day circulation test was conducted in the Hot Dry Rock (HDR) Phase II reservoir at Fenton Hill, New Mexico in May-June, 1986, where cold water was injected and hot water was recovered under high pressures, cooled and reinjected (Hendron, 1987). A total of 37,000 m^3 (9.76 million gal) of water was injected into the injection well (EE-3A) while a total of 23,000 m^3 (6.15 million gal) of hot water was produced from the production well (EE-2). The surface injection rates ranged up to 0.0265 m^3/s (420 gpm) although most of the pumping was done at rates of 0.0106 m^3/s (168 gpm) and 0.0185 m^3/s (294 gpm) with the surface pressures around 26.9 MPa (3900 psi) and 30.3 MPa (4400 psi) respectively. The production surface pressure was controlled around 3 MPa (4500 psi), resulting in surface production flow rates from 0.0063 m^3/s (100 gpm) to 0.0139 m^3/s (220 gpm).

The production well temperatures increased throughout the test, reaching a maximum of 192°C near the end of the test. The production power showed a corresponding increase, reaching a maximum of 10 MW_t after 28 days. The power increase resulted from the rise in production temperature combined with a rise in production rate.

The bottom-hole injection well pressure did not change much with injection rate or time, indicating fracture inflation and stimulation near the injection wellbore. The production rate from EE-2 showed an overall increasing trend. The overall reservoir impedance decreased throughout the test, resulting largely from the stimulation of the injection well. The injection well impedance decreased from 0.72 GPa s/m^3 (6.6 psi/gpm) to .002 GPa s/m^3 (0.02 psi/gpm) during the early part of the test due to near-wellbore cooling and pressurization. However, the decrease in the production well impedance was only a minor portion of the overall impedance, indicating that future improvement strategies should concentrate on the production well.

The rate of water loss decreased throughout the test, starting around 70% after 4 days of pumping and reducing to 26% after 30-days of pumping. The apparently high water loss values during the early portion of the test were caused primarily by reservoir inflation. Of the total injected water, 66% was recovered during this test and a further 20% was recovered during a subsequent vent-down.

II. PRESSURE-RATE RESPONSE

The injection-well pressures and flow rates are shown in Figure 1. Several experiments were carried out during the test, including many flow rate and pressure changes and shut-ins in both EE-3A and EE-2, as well as several vents from EE-2. The bottom-hole injection pressures were calculated from the surface data by correcting for temperature dependent pipe friction and hydrostatic head. These pressures changed only slightly with flow rate or with time, indicating flow through inflated fractures. With the assumption of turbulent flow through parallel fractures, pressures are proportional to the square root of the flow rate, as shown in Figure 2. Extrapolated back to zero flowrate, the curves for this experiment (2067) yield a bottom-hole fracture closure pressure of 55.6 MPa (8070 psi). As shown in Figure 2, this value is lower than that obtained from previous tests in the same

depth interval. This suggests that significant volumes of water went into the connections created by previous tests. In Figure 2, data for this test are grouped in two sets: one group taken at the start of the test, and another consisting of data obtained during later steady flows. The slope for this later data set is lower than the early set indicating reduced flow resistance. The production pressure and flow rate data are summarized in Figure 3. The pressure was generally maintained between 1.4 and 3.4 MPa (200 and 500 psi) to keep single-phase flow in the wellbore. It took approximately 4.25 hours to observe a significant pressure response in EE-2 after the start of injection into EE-3A. The production flow rate increased relative to steady injection flow rate due to reservoir inflation and an overall decreasing impedance.

After 30 days of pumping, both wells were shut in (Figure 4). Data for each well were analyzed using the Horner technique. While caution must be exercised in applying conventional petroleum engineering techniques to fracture-dominated reservoirs, a permeability-thickness product (kh) of 3 x 10^{-14} to 5 x 10^{-14} m^3 (100-150 md ft) is obtained for the region near the EE-2 production well. The skin factor "s" at EE-2 has a maximum value of -2. The variability of results near EE-2 is because there was virtually no wellbore storage effect. Similar calculations for the injection region yield a permeability-thickness product of 2 x 10^{-12} m^3 (7,800 md ft) and a skin factor of -15. The negative skin factors are consistent with the expected presence of fractures near the wellbores, and the permeability-thickness products are of the same order of magnitude as indicated by near-wellbore impedance (see Section IV). Also, the higher values of kh and more negative values of "s" for the injection well as compared to the production well are consistent with the stimulation at the injection well.

The extrapolated equilibrium reservoir pressure from Horner plots was 6.48 MPa (9400 psi) bottom-hole. Using an overall compressibility of 3 x 10^{-5} MPa^{-1} (2 x 10^{-7} psi^{-1}) and a integrated water-loss volume of 13,678 m^3 (3.61 million gal), a total reservoir volume of 16.3 x 10^6 m^3 (4,300 million gal) can be derived. This leads to a fracture volume porosity of 0.08%. This is in the range of values reported by Robinson and Jones (1987).

Fracturing pressures versus depth for this test (labeled "ICFT") are presented in Figure 5 along with data from previous flow tests. The new values follow the same general trend with depth, falling around a pressure gradient of about 19 MPa/km (0.8 psi/ft) (Kelkar et al., 1986). Also, the fracture closure stress obtained from the shut-in data is lower than that extrapolated from the ISIP method (Hickman and Zoback, 1981), again remaining consistent with previous results.

III. THERMAL BEHAVIOR AND POWER PRODUCTION

Surface production temperature was monitored throughout the test. Several temperature surveys were also run in each wellbore. Simulations of both EE-3A and EE-2 performance were made using a wellbore heat transfer (WBHT) code (Dash and Zyvoloski, 1982) that solves the basic 2-D radial equations for heat transfer, and accounts for forced convection in the wellbore and annulus, and for conduction to the surrounding rock mass. The results were in good agreement with field measurements as shown in Figure 6.

Analysis of the EE-3A wellbore surveys (Figure 7) shows that fluid exited the wellbore between 3530 - 3660 m (11,580-12,000 ft). Possible discrete fractures noted at 3530 m (11,580 ft), 3580 m (11,750 ft) and 3640 m (11,950 ft), are equivalent to fractures first stimulated in previous tests.

EE-2 production temperature was modeled using a reservoir outlet temperature of 232°C (this corresponds to the original rock temperature at 3535 m (11,600 ft)) and is in good agreement with Kuster temperature surveys run during the test (Figure 8). It was impossible to precisely identify fracture inlets since EE-2 could not be logged below 3200 m (10,500 ft).

The post-experiment Kuster survey (Figure 8) shows a flat, hot profile up to 2990 m (9,800 ft) indicating a small amount of fluid, about 0.0019 m^3/s (30 gpm), was still entering the wellbore below that depth after shut-in, flowing up the wellbore and out into the rock at 2990 m. The flat portion of the curve from 610 to 800 m (2,000-2,625 ft) corresponds to an aquifer near the transition of the sediments and Pre-Cambrian basement rock.

Thermal power production was estimated using the measured production temperature at EE-2 wellhead, injection temperature at EE-3A and the measured flow rate through the heat exchangers. A peak power of about 10 MW_t was estimated. The power production of 9.2 MW_t at the end of the test was consistent with model projections for a sustained flow rate of 0.0126 m^3/s (200 gpm) and a 192°C production temperature. Projection of performance trends during the test, assuming no thermal drawdown in the reservoir, indicate that from 10-12 MW_t could be produced after one year if the flow rate is maintained between .0126 m^3/s - .0158 m^3/s and production temperature is 200-210°C.

IV. IMPEDANCE AND WATER LOSS

Impedance is determined by dividing the pressure drop across a flow segment by the production flow rate. Figure 9 shows the total

reservoir impedance, corrected for buoyancy and friction effects in the wellbores, decreased from 7 GPa·s/m^3 (64 psi/gpm) to 2 GPa·s/m^3 (18 psi/gpm) over the 30-day test. The most rapid decline occurred during the first week of injection due to hydraulic and thermal stimulation near the injection wellbore.

Near-wellbore impedance is found by subtracting the flowing surface pressure from the instantaneous shut-in pressure, correcting this amount for buoyancy and friction, and then dividing by the surface flow rate immediately prior to the shut-in. The injection well impedance dropped rapidly during the first half of the test from 0.7 GPa·s/m^3 (6.6 psi/gpm) to 2 x 10^{-3} GPa·s/m^3 (0.02 psi/gpm).

Water loss rate, defined as the ratio of the difference between the injected and recovered water to the amount injected at a given time, is shown in Figure 10. There were four mechanisms of water loss operating during the flow test: 1) reservoir extension indicated by micoseismic activity; 2) inflation of the reservoir; 3) flow into an older reservoir system; and 4) diffusion into secondary porosity (i.e. into the country rock surrounding the fracture). The largest water loss rate, about 70%, occurred near the beginning of the test as the formation inflated. As the reservoir approached equilibrium, water loss averaged 30% of the injected volume, with a low of 26%.

Adjacent to the reservoir currently under testing, there is an older, shallower reservoir, termed Phase I, at depths around 2600-2700 m (8,500-8,900 ft) (Dash et al., 1983). The wells in this older reservoir were used as pressure taps during this test. After 28 days of pumping into EE-3A, the older wells experienced a pressure rise from atmospheric to 0.83 MPa (120 psi). This pressure rise was modeled by representing the as a sphere of constant pressure, embedded in an infinite homogeneous medium surrounding it, resulting in a regional permeability of 18 x 10^{-18} m^2 (18 microdarcies). This compares well with previous estimations of 5 x 10^{-18} m^2 to 10 x 10^{-18} m^2 (5 to 10 microdarcies).

V. COMPARISON WITH OTHER HDR RESERVOIRS

There are two other HDR reservoirs that have been subjected to circulation testing where significant quantities of thermal energy were extracted by circulation of water. One of these was the Phase I reservoir at Fenton Hill, USA (Dash et al., 1983). The other is the British reservoir currently being tested at Rosemanowes Quarry in Cornwall, Great Britain (Bachelor, 1984). A comparison of these two reservoirs with the Phase II reservoir is given in Table I. The data shown in this table represent 30 days of operation for all three reservoirs. Note that the Phase II reservoir under discussion is significantly hotter and larger than the Phase I reservoir. Both the Phase I US reservoir and the British reservoir have shown considerable improvement over time beyond the 30-day comparison here. Thus, based on the limited experience to date, it is likely that the performance of the Phase II US reservoir will improve during subsequent long term tests.

CONCLUSIONS

A 30-day circulation test was carried out during which the production flow rate, temperature and thermal energy extraction showed increasing trends. Based on thermal modeling, an energy production rate around 12 MW_t could be expected at the end of one year. The reservoir flow resistance declined from 7 GPa·s/^{3} to 2 GPa·s/m^3 and the fraction of water recovered during the test increased from 30% to 74%. Comparison with other HDR reservoirs leads to the possibility of further improvement of performance parameters over longer periods. The hydraulic behavior of the reservoir shows that future improvement strategies should be focused on the production well.

ACKNOWLEDGMENTS

This work is being supported by the US Department of Energy. Authors would like to acknowledge several fruitful discussions with Robert Potter, Hugh Murphy and Gerald Jones of Los Alamos National Laboratory. Thanks are due to Ms. Bonita Busse for typing the text and to John Paskiewicz and Ruth Robichaud for preparation of figures.

REFERENCES

Bachelor, A.S., 1984, "Hot Dry Rock Geothermal Exploration in the United Kingdom," Modern Geology, v9, pp 1-41.

Dash, Z.V. and Zyvoloski, G., 1982, "Problems Associated with Application of a Wellbore Heat Transmission Computer Code", Eighth Workshop on Geothermal Reservoir Engineering, Stanford, California.

Dash, Z.V., Murphy, H.D., Aamodt, R.L., Aguilar, R.G., Brown, D.W., Counce, D.A., Fisher, H.W., Grigsby, C.D., Keppler, M., Laughlin, A.W., Potter, R.M., Tester, J.W., Trujillo, P.E., and Zyvoloski, G.A., "Hot Dry Rock Geothermal Reservoir Testing 1978 to 1980," J. Volcan. Geother. Res., v. 15, pp. 59-99, 1988.

Fisher, H.F., 1980, "The Pressure Transient Testing of a Manmade Fractured Geothermal Reservoir: An Examination of Fracture Versus Matrix Dominated Flow Effects", Los Alamos National Laboratory Report LA-8536 MS

Hendron, R.H., 1987, "The US Hot Dry Rock Project," Proceedings, Twelfth Annual Workshop on Geothermal Reservoir Engineering, Stanford, California.

Hickman, S.M., and Zoback, M.D., 1981, "Interpretation of Hydraulic Fracturing Pressure-Time Data for In-Situ Stress Determination," Proceedings of a Workshop on Hydraulic Fracturing Stress Measurements, National Academy Press, Washington, D.C.

Kelkar, S.M., Murphy, H.D., and Dash, Z.V., 1986, "Earth Stress Measurements in Deep Granitic Rock," Proceedings, 27th US Symp. Rock Mech., University of Alabama.

Robinson, B.A., and Jones, G.F., 1987, "A Tracer-Based Model for Heat Transfer in a Hot Dry Rock Reservoir," Geothermal Resources Council Annual Meeting, Nevada.

TABLE I

COMPARISON OF THREE HDR RESERVOIRS
AFTER ONE MONTH OF OPERATION

	FENTON HILL ENLARGED PHASE I RESERVOIR	FENTON HILL CURRENT PHASE II RESERVOIR	ROSEMANOWES CORNWALL, UK
Depth of Reservoir, m	2,800	3,550	2,400
Temperature of Reservoir, °C	195	240	85
Modal Volume, m^3	160	350	270
Surface Temperature, °C	135	191	76
Thermal Power, MW_t	3	9	1
Production Flow Rate, m^3/s	0.007	0.013	0.004
Injection Well Pressure, MPa	10	30	4
Corrected Impedance GPa s/m^3	1.7	2.2	1.0
Water Loss Rate at 30 Days, m^3/s	0.0011(16%)	0.006(33%)	0.0004(10%)

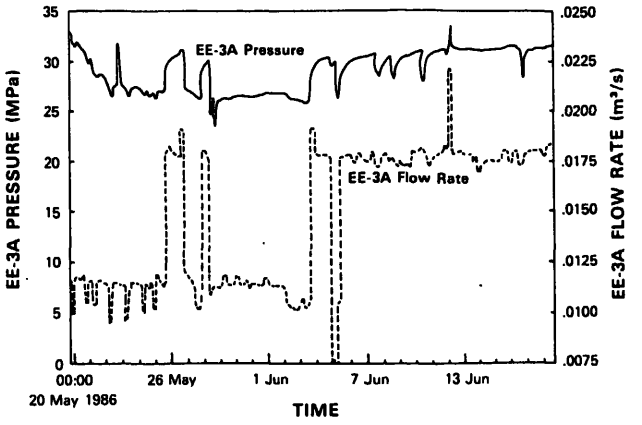

Figure 1. Surface pressure and flow rate at injection well.

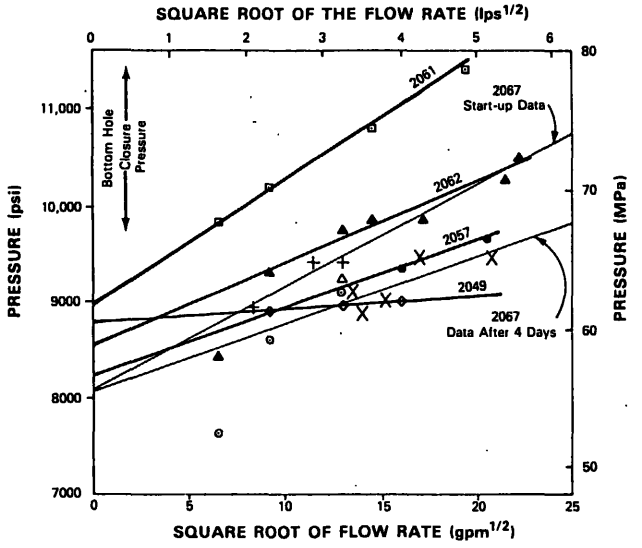

Figure 2. Bottom hole fracture closure pressure for this experiment (2067) along with previous data.

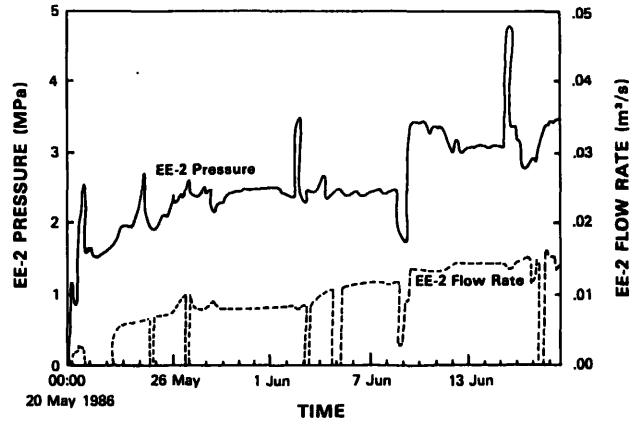

Figure 3. Surface pressure and flow rate at production well.

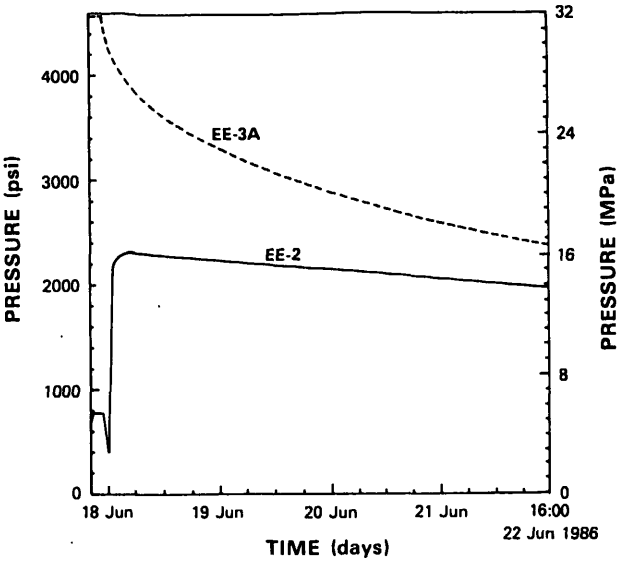

Figure 4. Pressure response during final shut-in at injection and production wells.

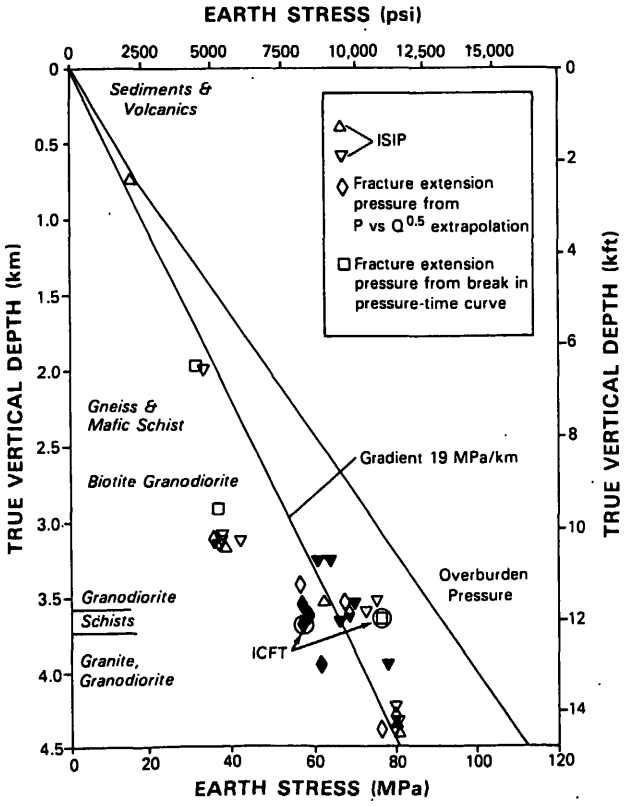

Figure 5. Fracture extension pressure for this experiment (2067) along with previous data.

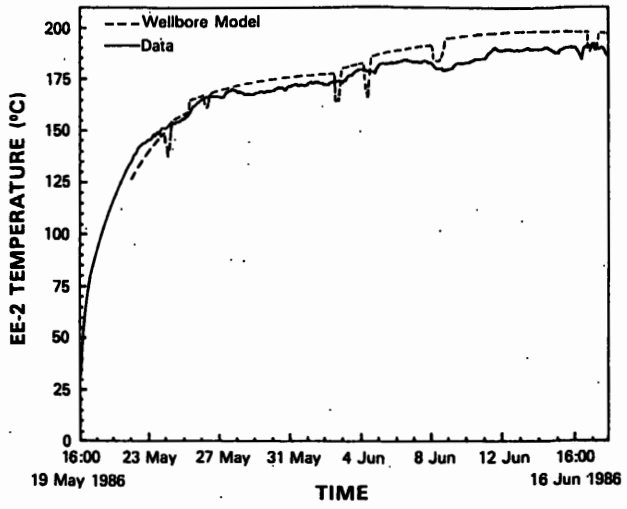

Figure 6. Surface temperature for production well along with model predictions.

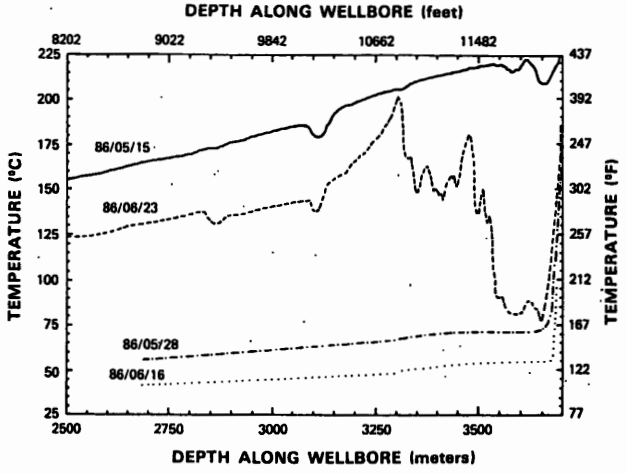

Figure 7. Injection well temperature surveys taken before (86/05/15), during (86/05/28, 86/06/16) and after (86/06/23) flow test.

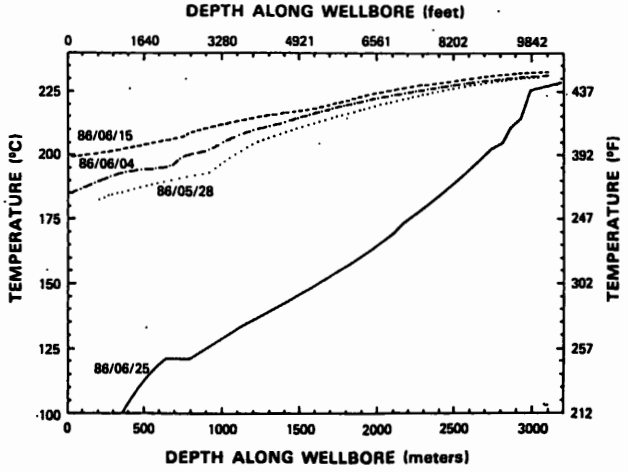

Figure 8. Production well temperature surveys taken during (86/05/28, 86/06/04, 86/06/15) and after (86/06/25) flow test.

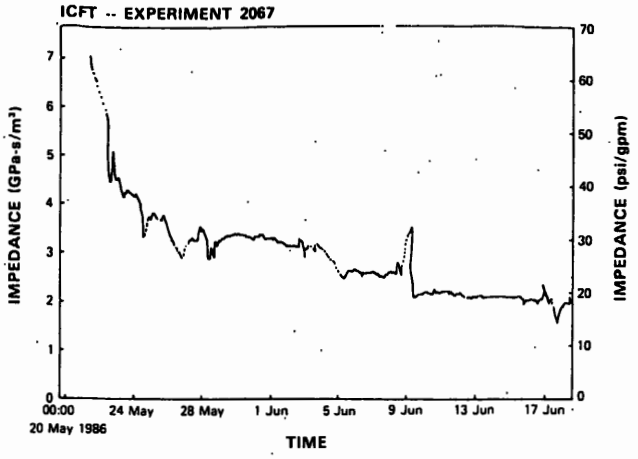

Figure 9. Overall reservoir impedance.

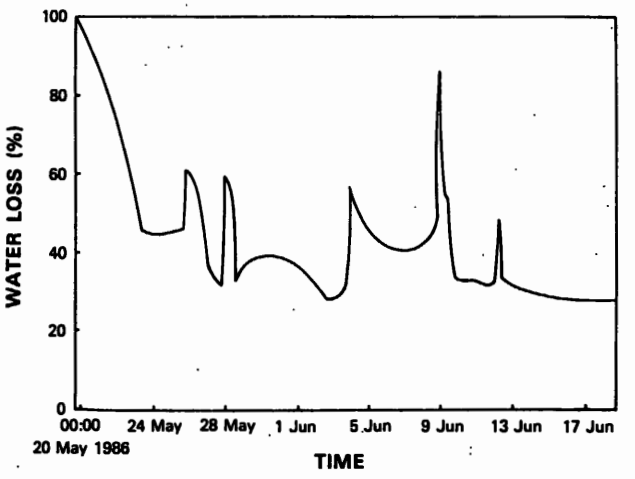

Figure 10. Percent water loss.